10/12-26-90 JSD

UCRL-ID-104867

Anatomy of a Disruption in MTX

E. B. Hooper, T. A. Casper, C. J. Lasnier,
M. A. Makowski, W. H. Meyer, J. M. Moller,
K. Oasa, B. W. Rice, R. D. Wood

Report of ITER R&D Contribution
Task PH07

October 15, 1990

Lawrence Livermore National Laboratory

This is an informal report intended primarily for internal or limited external distribution. The opinions and conclusions stated are those of the author and may or may not be those of the Laboratory.
Work performed under the auspices of the U.S. Department of Energy by the Lawrence Livermore National Laboratory under Contract W-7405-Eng-48.

MASTER

DISTRIBUTION OF THIS DOCUMENT IS UNLIMITED

DISCLAIMER

This document was prepared as an account of work sponsored by an agency of the United States Government. Neither the United States Government nor the University of California nor any of their employees, makes any warranty, express or implied, or assumes any legal liability or responsibility for the accuracy, completeness, or usefulness of any information, apparatus, product, or process disclosed, or represents that its use would not infringe privately owned rights. Reference herein to any specific commercial products, process, or service by trade name, trademark, manufacturer, or otherwise, does not necessarily constitute or imply its endorsement, recommendation, or favoring by the United States Government or the University of California. The views and opinions of authors expressed herein do not necessarily state or reflect those of the United States Government or the University of California, and shall not be used for advertising or product endorsement purposes.

This report has been reproduced
directly from the best available copy.

Available to DOE and DOE contractors from the
Office of Scientific and Technical Information
P.O. Box 62, Oak Ridge, TN 37831
Prices available from (615) 576-8401, FTS 626-8401.

Available to the public from the
National Technical Information Service
U.S. Department of Commerce
5285 Port Royal Rd.,
Springfield, VA 22161

Price Code	Page Range
A01	Microfiche
Papercopy Prices	
A02	1- 10
A03	11- 50
A04	51- 75
A05	76-100
A06	101-125
A07	126-150
A08	151-175
A09	176-200
A10	201-225
A11	226-250
A12	251-275
A13	276-300
A14	301-325
A15	326-350
A16	351-375
A17	376-400
A18	401-425
A19	426-450
A20	451-475
A21	476-500
A22	501-525
A23	526-550
A24	551-575
A25	576-600
A99	601 & UP

UCRL-ID--104867

DE91 004992

ANATOMY OF A DISRUPTION IN MTX*

E. B. Hooper, T. A. Casper, C. J. Lasnier, M. A. Makowski, W. H. Meyer, J. M. Moller, K. Oasa[(a)], B. W. Rice, R. D. Wood

Lawrence Livermore National Laboratory
Livermore, CA 94526 USA

October 15, 1990

INTRODUCTION

Disruptions are observed in the Microwave Tokamak Experiment, MTX (née Alcator C), over a wide range of plasma parameters. Indeed, disruptions often occur far from the boundaries of the operating space as defined by Hugill and l_i-q plots. [1] Despite this, the general behavior during the disruptive process is generally similar whatever the operating parameters. This report will describe one disruption in detail in order to provide a detailed anatomy of the event.

Observation of many disrupting discharges has provided several general results:

- The MHD activity before disruptions has various forms. Disruptions are seen in which: (A) No MHD activity is seen; (B) m=2 activity is seen; and (C) m=2 and m=3 activities are seen. For the data to date, the toroidal mode numbers are ambiguous, but consistent with 2/1 and 3/2 modes. Coils for locked modes were not available during these measurements, but have been installed for future experiments.

- The strongest MHD activity is seen at low q (<3.5), but disruptions without precurser activity are seen at all q.

- The Hugill (density) limit is generally not disruptive, but rather behaves as if gas penetration and/or particle confinement are reduced. [2]

- Following an initial disruption, current channel usually reforms at reduced major radius, and the plasma reheats implying that the flux surfaces have closed. The new configuration is unstable, however, and the channel disrupts at least once more as the plasma is lost.

To see the detailed behavior we turn to a particular discharge.

GENERAL DESCRIPTION OF A DISRUPTIVE DISCHARGE

Discharge 8670 was chosen for this study as a disrupting and relatively well diagnosed shot. Its behavior is characteristic of many of those disruptions in MTX resulting from startup problems and which are not near the density or low q limits. (As noted above, however, the disruption process itself does not appear sensitive to the triggering events.) The MTX tokamak was operated with R_0 = 0.64 m, a = 0.165 m, and B_t = 4.9 T. The discharge current and line-averaged density are shown in Fig. 1. Note that the discharge ended in a series of three disruptions just before 0.2 second.

A contour plot of the line-averaged soft-xray emission, Fig. 2a, shows several features of note. We see that during the buildup stage the discharge shows evidence of minor disruptions; operation at this low density is difficult in MTX. The strong drop in x-ray intensity at 0.06 s, reflected in rapid changes in the discharge current and density, probably resulted from MHD activity although loop data is not available for that time interval for this discharge.

There was a burst of heavy impurity simultaneously with this first drop in xrays, as seen in Fig. 2b. The level then apparently drops significantly while the electron temperature rises; the grating in the spectrometer would not have seen higher ionization states, however, and it is possible that the states shown in the figure burned out. The light impurity density rose later in the shot as it headed towards disruption.

It is also noteworthy that sawteeth were never established in this discharge. The value of $q(0)$ calculated from the electron temperature (assuming the current to be in equilibrium with T_e) was slightly above one as shown in Fig. 3. However, from about 0.13 to 0.17 s, the discharge was well behaved. Electron temperature profiles show a steepening of the profile after about 0.16 s, arising primarily from an increase in central T_e. We will examine the behavior after this in more detail below; however, we can see from the contour plot, Fig. 2a, that there is precursor x-ray activity before the disruption, and that following the disruption at 0.185 s the plasma channel reforms twice at radii successively closer to the inner wall before being lost completely.

The discharge was far from the usual stability boundaries, as seen from the Hugill and l_i-q plots shown in Fig. 4. From both viewpoints, the discharge was in the middle of the normally stable operating space, consistent with the other indications that problems leading to the disruption arose during the plasma formation and in the early time behavior.

PREDISRUPTIVE BEHAVIOR

The electron temperature and soft x-ray emission are shown for the last 0.05 s of the discharge in Fig. 5. Prior to the actual disruption, there were three drops in x-ray

emission. No MHD (or other) modes were observed before or during these precurser events. However, simultaneous with them was an incoherent magnetic burst, shown in Fig. 6a. These events caused a rapid flattening of the electron temperature profile during the burst, as shown in the two time traces of Figs. 6b and 6c and in the contour plots of Fig. 5. We see from Fig. 6 that the maximum electron temperature changes near the axis and edge were about 20% with an inversion radius at about 8 cm. We estimate from the electron temperature profile that $q(r=8) \approx 1.8$, so the event plausibly occurred at the q=2 surface. After each precurser event, the electron temperature recovers and its profile becomes increasingly more peaked.

Note from Fig. 7 that the discharge current did not change during these three events; a small negative voltage spike (–2 V) was seen on the loop voltage; during disruptions, –20 to –50 V are typical. Thus, the presumed magnetic reconnection was not extensive enough to disrupt the plasma. This observation supports the hypothesis that locked modes were involved.

Furthermore, both the line-averaged density, Fig. 7b, and the density contour plot, Fig. 8, show that the pre-disruptive events had only a small effect on the density profile. The events were thus predominantly internal rearrangements of electron temperature (and probably current density) which were not extensive enough to cause global plasma losses. They thus differ (in strength, at least) from the usual minor disruptions and appear more like sawteeth in nature.

The three precursor events and the first disruption occur with time spacings of 0.0060, 0.0050, and 0.0050 s. This time is comparable to both the energy confinement and resistive diffusion times. Just before the disruption the plasma kinetic energy is about 3.9 kJ and the ohmic heating about 600 kW, yielding an energy confinement time, $\tau_e \approx$ 6.5 ms. The resistive diffusion time is $\tau_R = \mu_o a^2 / \eta \approx 0.7 (r/a)^2 T_e^{3/2} / Z_{eff}$ s for a radius r; at 0.5 keV, 1/2 the peak electron temperature of 1 keV, $Z_{eff} \leq 2$ (c.f. Fig. 3), and a radius of order 1/4 the minor radius, this is 5-10 ms. Thus, the observed time between MHD events of 5-6 ms is consistent with the recovery time of the plasma.

The electron temperature profiles steepen after about 0.16 s; however, this is due to central heating. There is no evidence that impurity radiation near the plasma edge is narrowing the current channel as sometimes triggers disruptions. [3] The bolometers (not shown) also do not show an increase before the disruption.

THE DISRUPTION

The fourth MHD event, occuring at 0.185 s, caused the discharge to disrupt. As can be seen from the soft x-ray and temperature contours, Fig. 5, the current channel reformed at a smaller major radius, $R \approx 0.60$ m, disrupted a second time and reformed at $R \approx 0.56$ m, and then was lost completely. This process can be seen more clearly in Fig. 9 which shows the x-ray, electron temperature, and density profiles. Note that for both the

temperature and density data some channels were not working well, so the details are not as complete as for the xrays.

The current profile becomes less peaked relative to the reduced minor radius when the plasma moves nearer the inner wall. The force balance requires a vertical field,

$$B_v = \frac{\mu_o I}{4\pi R_o}\left[\beta_p + \frac{l_i}{2} - \frac{3}{2} + \ln\left(\frac{8 R_o}{a}\right)\right] .$$

The change in the discharge current, I, following each of the first two disruptions is about 25%, and the vertical field, B_v, remains unchanged. At constant vertical field,

$$\frac{\Delta I}{I} = \frac{\Delta R_o}{R_o} - \frac{\Delta(\beta_p + l_i/2) + \Delta R_o / R_o - \Delta a / a}{\beta_p + l_i/2 - 3/2 + \ln(8 R_o / a)} .$$

We estimate from Fig. 4b that just before the first disruption, $\beta_p + l_i/2 = 0.65$. (Beta only contributes a small correction.) Thus, a reduction in a and corresponding inward movement in R_o of 4 cm can only account for about half of the change in current. The new force balance will require an increase in $\beta_p + l_i/2 \approx 0.3$ and thus a relative narrowing of the current channel. This will drive the plasma toward and probably above the maximum value of l_i at which a stable MHD equilibrium can be established; c.f. Fig. 4.

The collapse of the temperature during the disruption was very fast: Fig. 10 shows the temperature change on axis measured by the ECE. The instrument had a 100 kHz filter in the electronics; the measured time-of-change of about 20 μs is therefore only an upper limit and the actual time may be faster. The fast (JAERI) soft xrays, Fig. 11, show the collapse time averaged over the entire plasma. The full (x-ray decay) time for the first disruption was about 150 μs; for the final event in which the plasma was lost, the time was only 50 μs.

Temperature profiles just before (0.185 ms) and just after (0.186 ms) are shown in Fig. 12. It is not certain that the peak (at r = – 3.7 cm) before the disruption is real as the right-hand 3 points were limited by bit noise and thus have a low accuracy. In any event, the temperature dropped across the entire profile, including the plasma edge.

DISCUSSION

The electron temperature will collapse during the disruption due to rapid diffusion in the (putative) stochastic magnetic field. If the electron step size (islands) is δ, the diffusion time [4] is $\tau_\chi \approx (q\, R/v_{te})\,(a/\delta)^2$, with v_{te} the electron thermal velocity. The temperature drops to about 0.2 keV across the entire plasma (Fig. 6b), so if $a/\delta \approx 10$, $\tau_\chi \approx 7\times10^{-6}\, T_e^{-1/2} \approx 1.5\times10^{-5}$ s, roughly as observed in Fig. 10.

In these discharges, the electrons and ions are closely coupled. The equilibration time is $\tau_{eq} \approx 10^{-2}\, T_e^{3/2} / n_{20}$; at $T_e = 0.2$ keV and $n_{20} = 1$, $\tau_{eq} \approx 9\times10^{-4}$ s. Thus, the ions provide a heat reservoir which can help reheat the electrons when the current channel reforms. In addition, of course, a full thermal model would also include ohmic heating and impurity radiation.

The series of disruptions with the plasma reforming but not maintaining stability are characteristic of events in MTX both with and without observed MHD activity. There is apparently a competition between the loss of current to the wall and the reformation of closed flux surfaces in the plasma. If well understood, the reforming of the current channel may offer an opportunity for recovering from the initial disruption: a fast coil on the inside major radius could be fired to drive the plasma back to the center of the vacuum vessel where it might be possible to form a new stable discharge.

REFERENCES

* This work was performed under the auspices of the U. S. Department of Energy by the Lawrence Livermore National Laboratory under contract W-7405-ENG-48.

(a) Permanent address: Japan Atomic Energy Research Institute. Work performed as part of Annex VI, US-Japan Implementing Agreement in Magnetic Fusion Energy.

1. E. B. Hooper and M. A. Makowski, "Characterization of Disruptions in the Microwave Tokamak Experiment, MTX", (Report of ITER R&D Contribution, Task PH07), UCRL-ID-103473, March 30, 1990.

2. M. Greenwald, J. L. Terry, S. M. Wolfe, S. Ejima, M. G. Bell, S. M. Kaye, G. H. Neilson, Nucl. Fusion **28**, 2199 (1988).

3. B. B. Kadomtsev, Plasma Phys. Control. Fusion **26**, 217 (1984).

4. J. Wesson, et al., Nucl. Fusion **29**, 641 (1989).

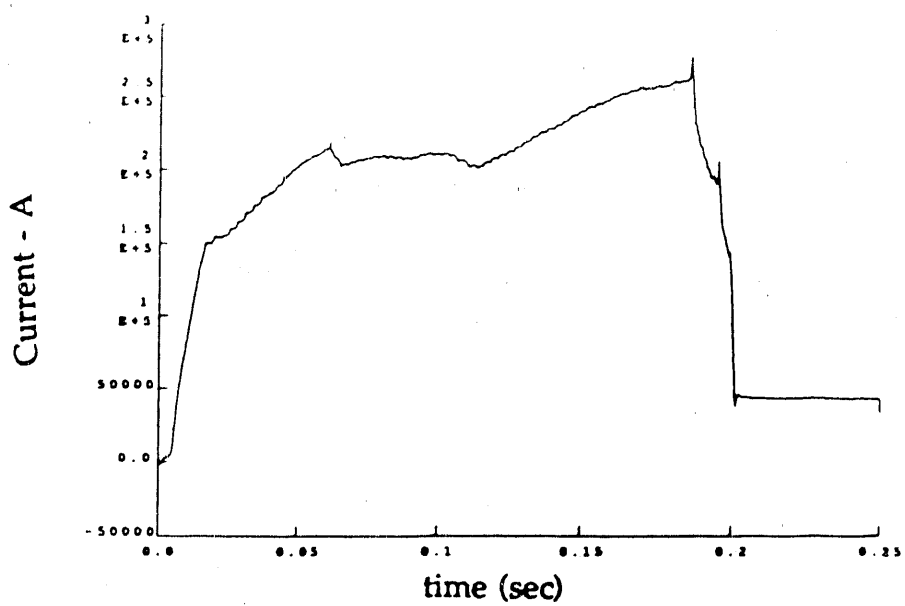

(a) Discharge Current, I

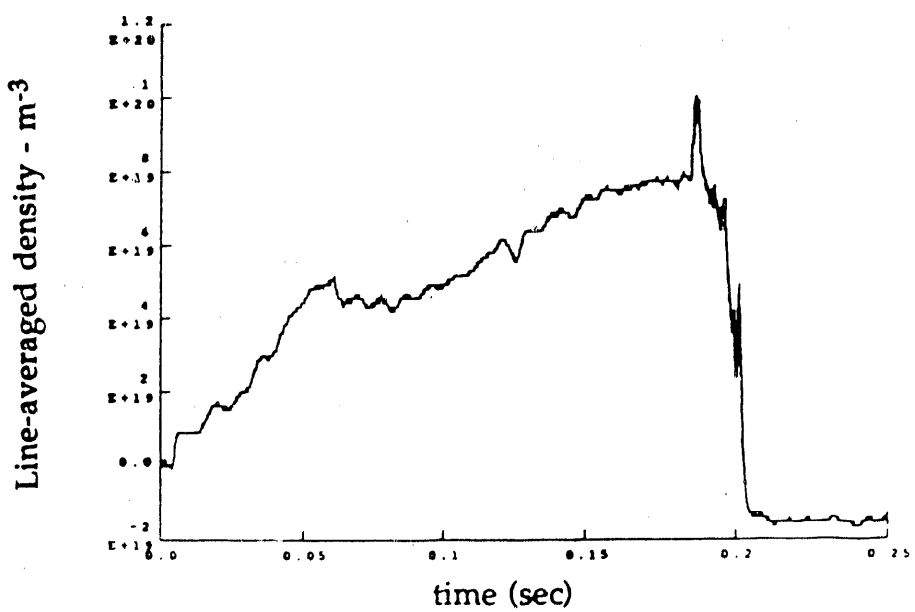

(b) Density, $\bar{n}$

Fig. 1 Shot 8670

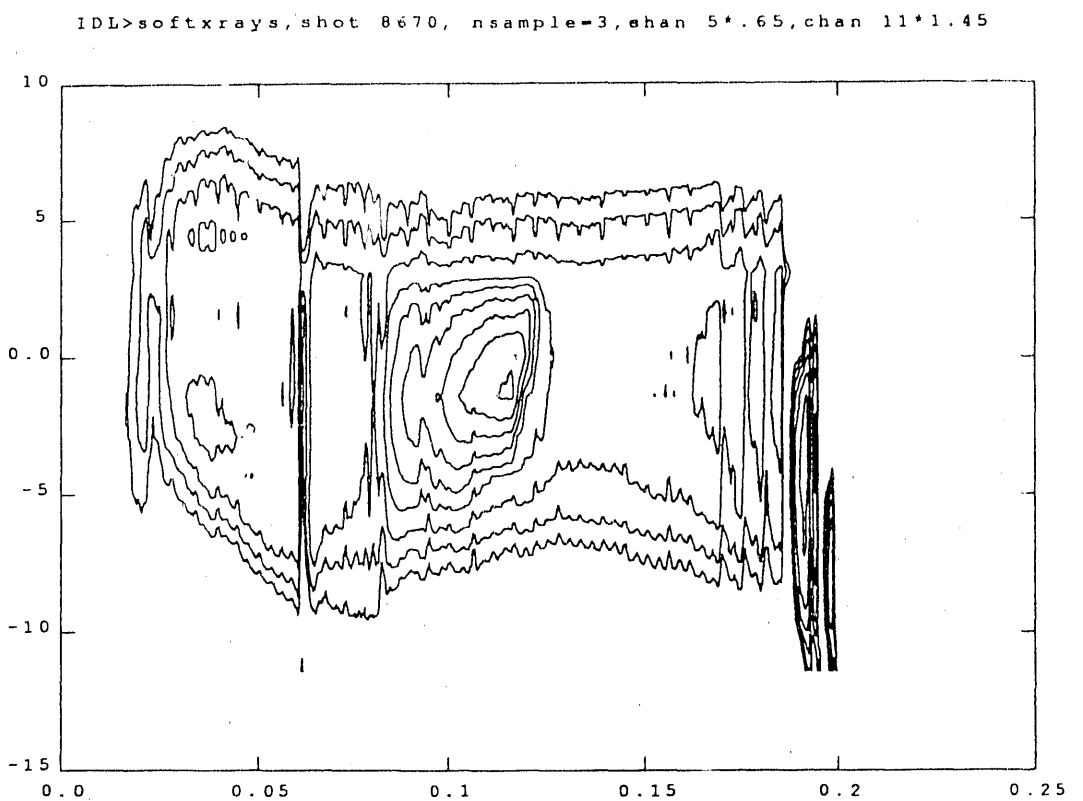

Fig. 2a Soft x-ray contours. Plotted are the line-integrated x-rays; contours spaced at intervals of $(2.0)^{\ell/2}$

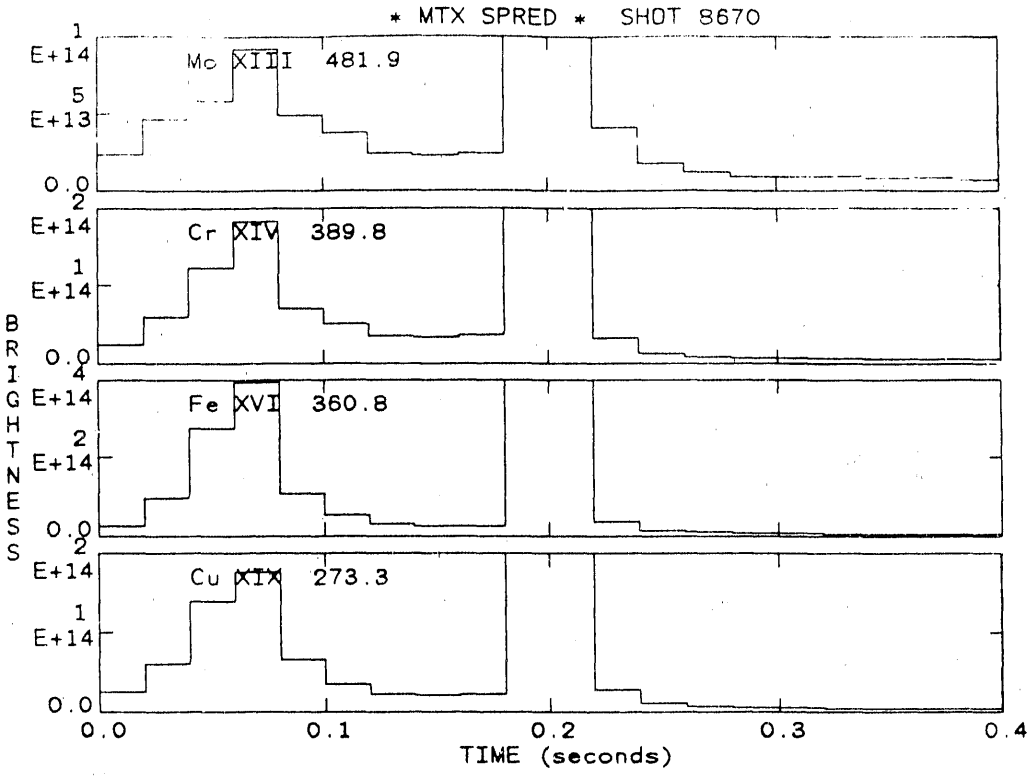

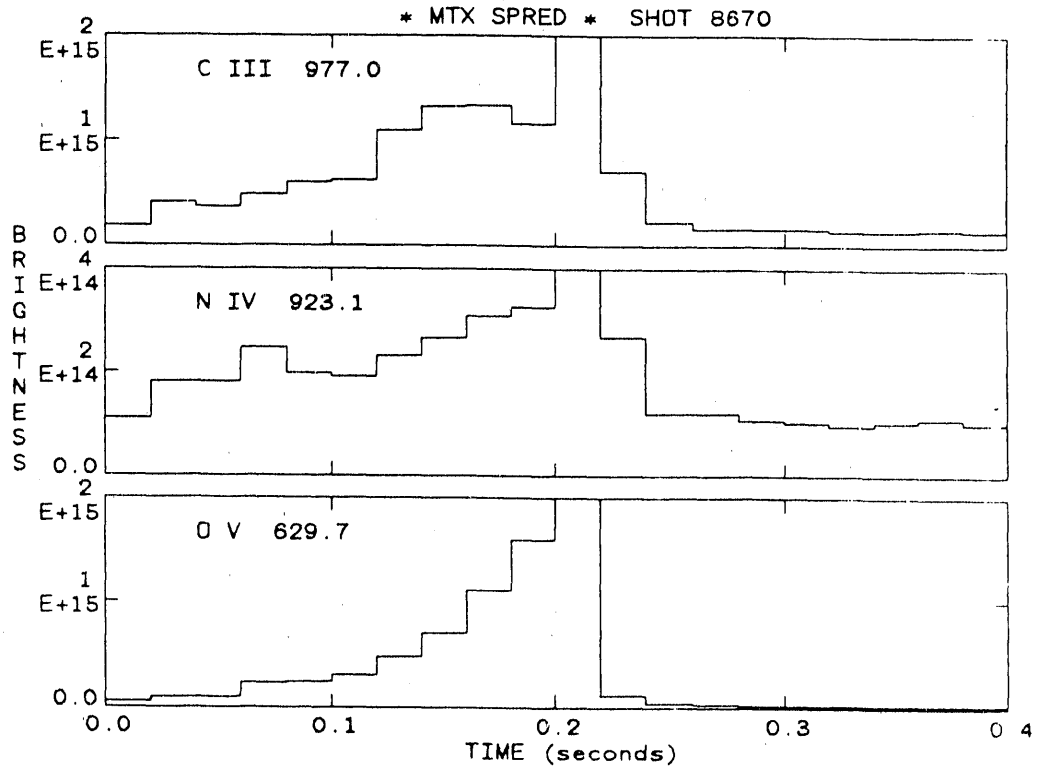

Fig. 2b Impurity behavior for selected lines

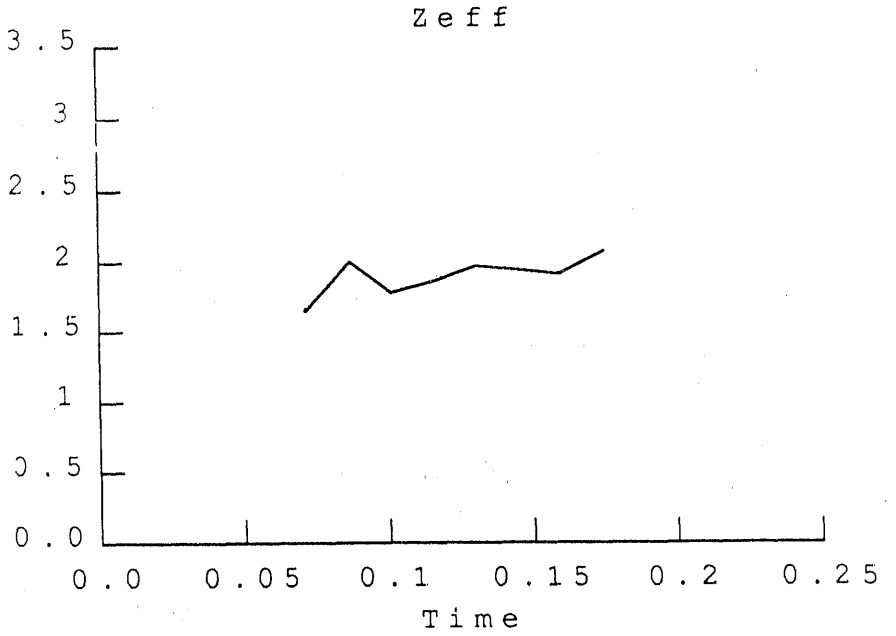

(a) Z_{eff} from visible bremsstrahlung

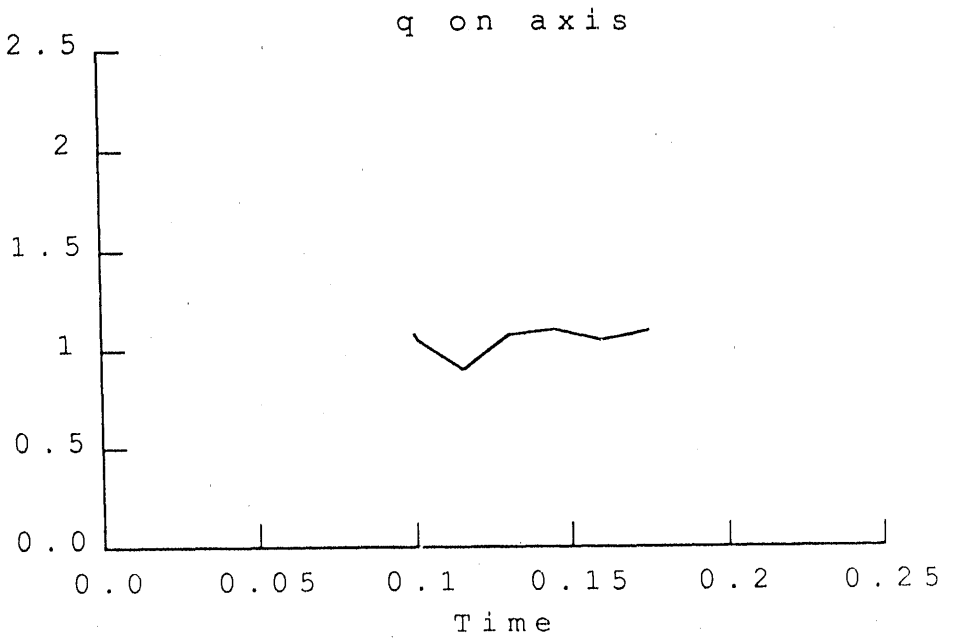

(b) $q\,(0) \sim T_e^{3/2}$, assuming the current and electron temperature are in equilibrium

Fig. 3

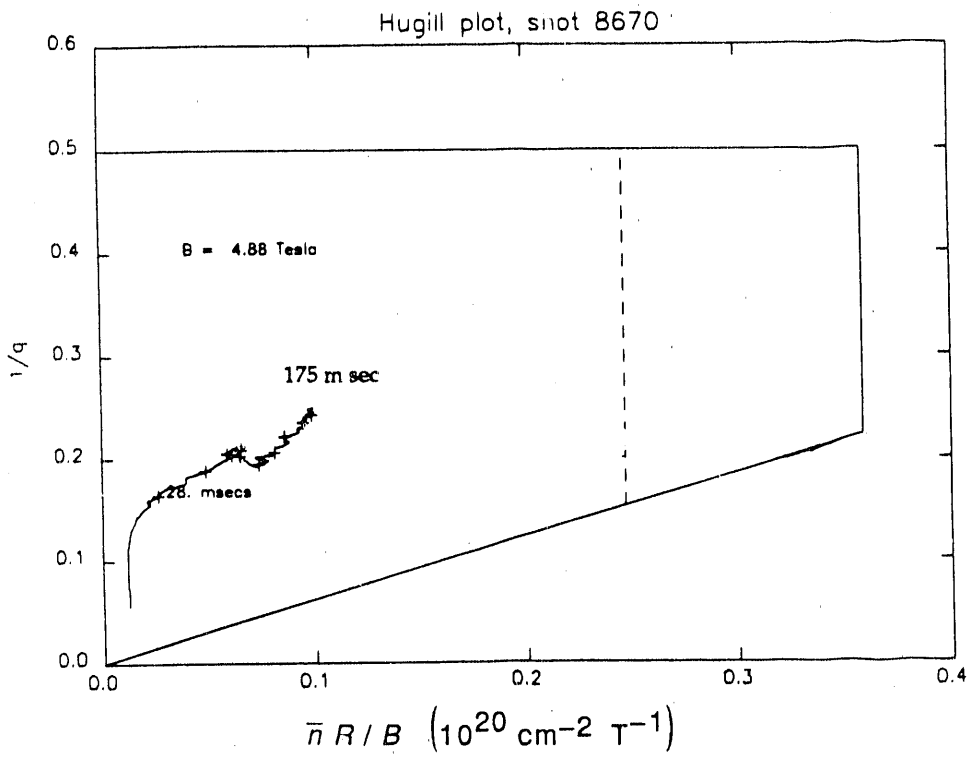

(a) Hugill plot

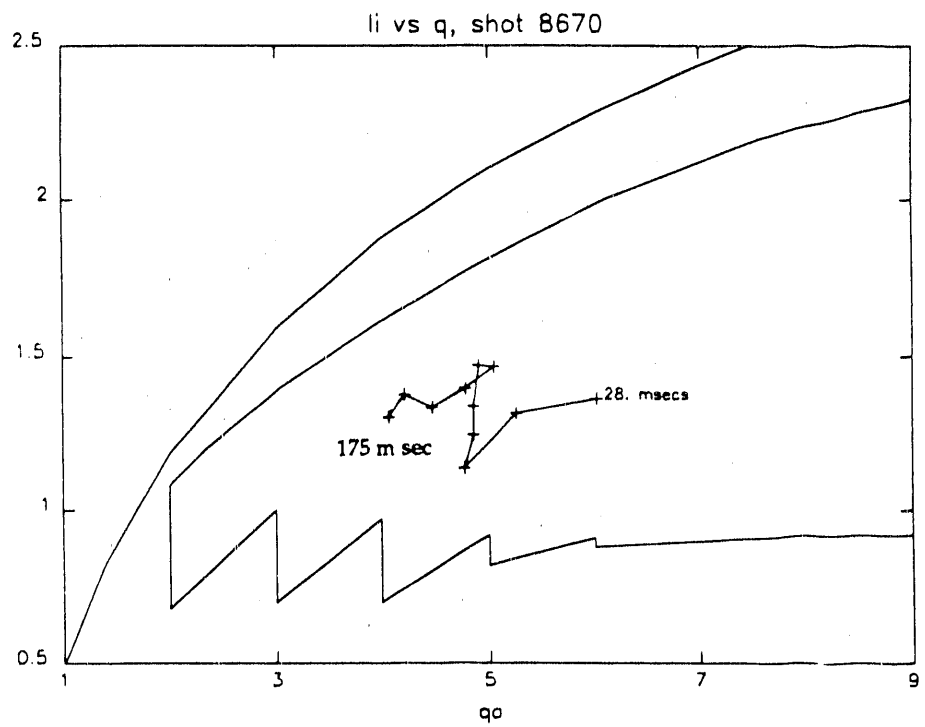

(b) l_i-q plot
The internal inductance is calculated assuming equilibrium with the electron temperature.

Fig. 4

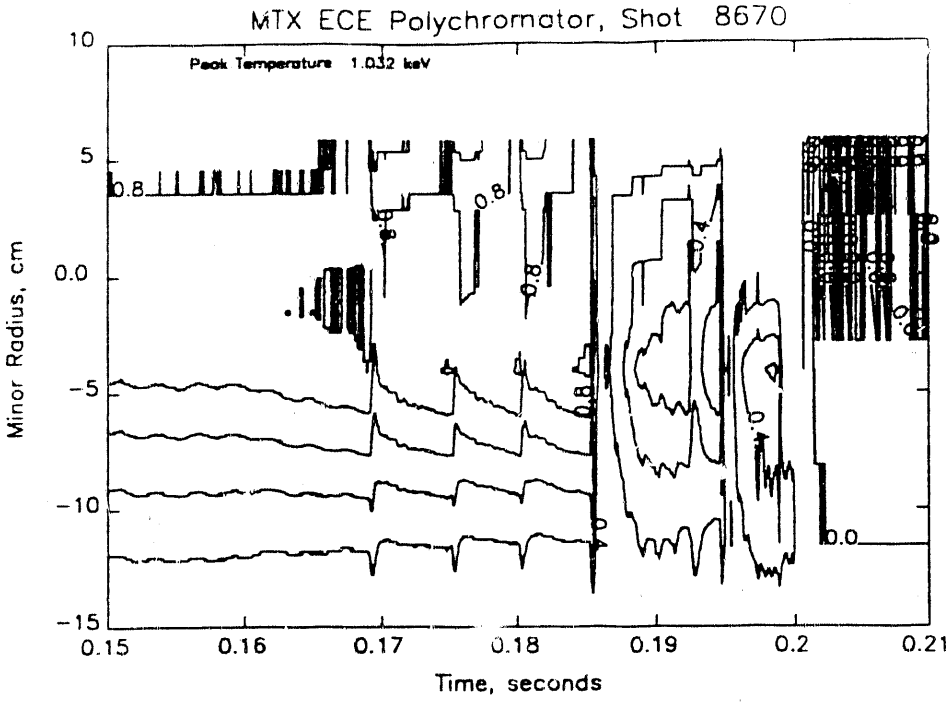

(a) Electron temperature from ECE. The channels at $r > 0$ were limited by bit-noise.

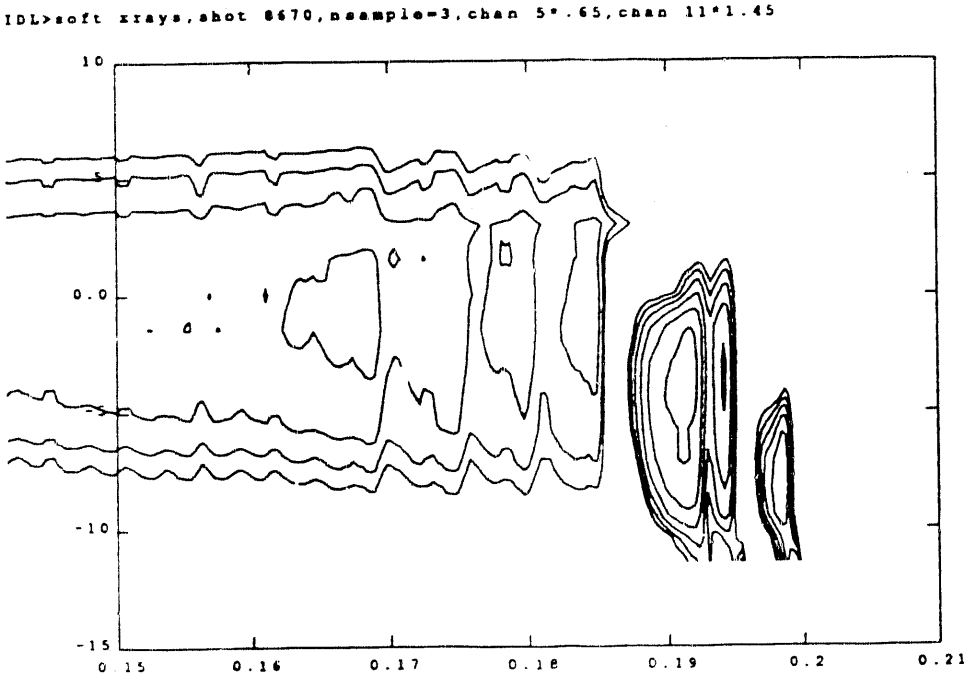

(b) Soft x-ray contours. (Chord integrated) contour spacing as in Fig. 2a.

Fig. 5

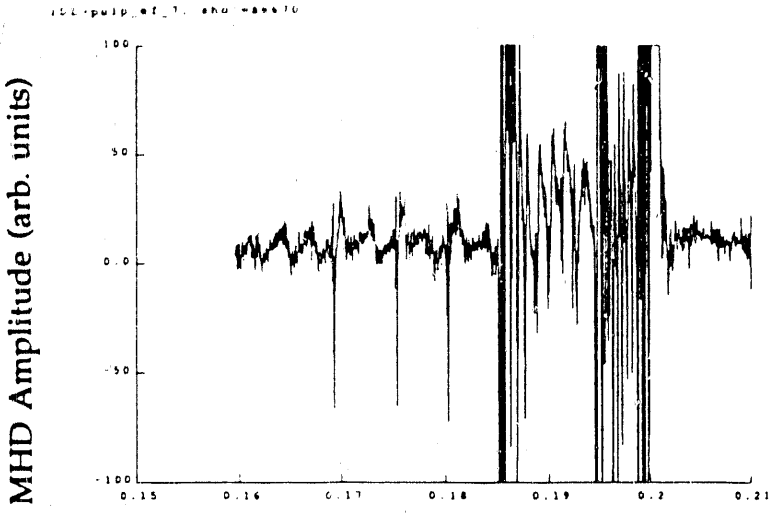

(a) Amplitude of MHD activity

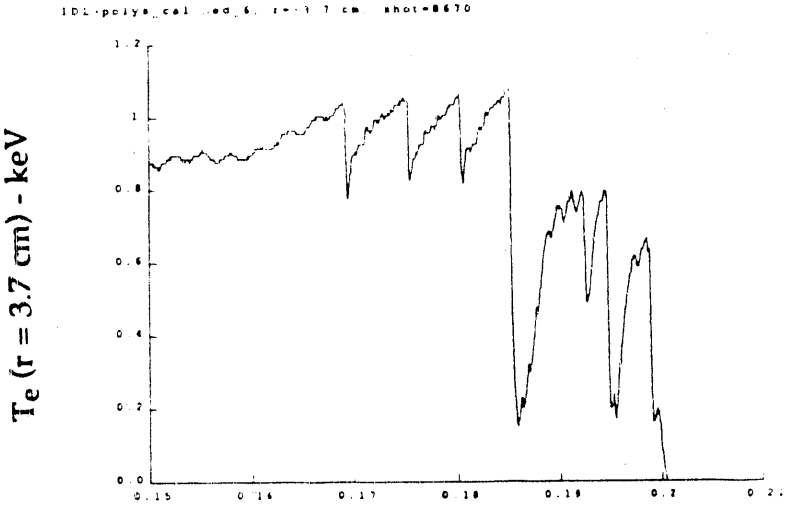

(b) Electron temperature from ECE at $r = -3.7$ cm.

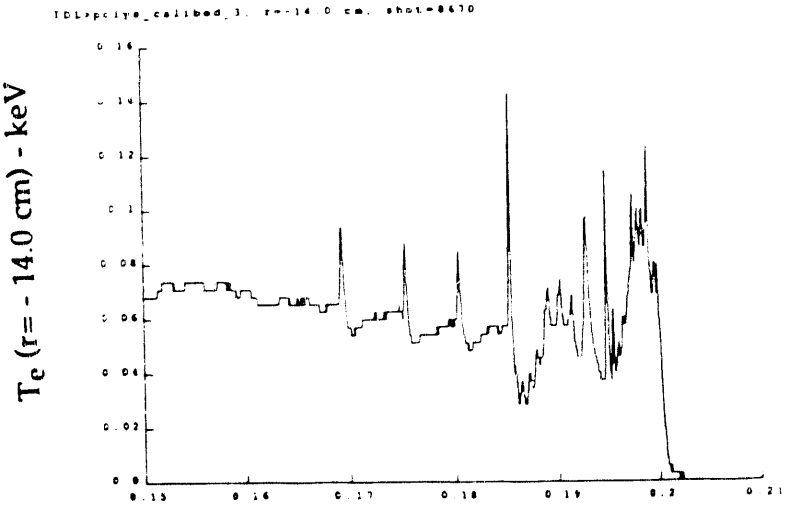

(c) Electron temperature from ECE at $r = -14.0$ cm.

Fig. 6

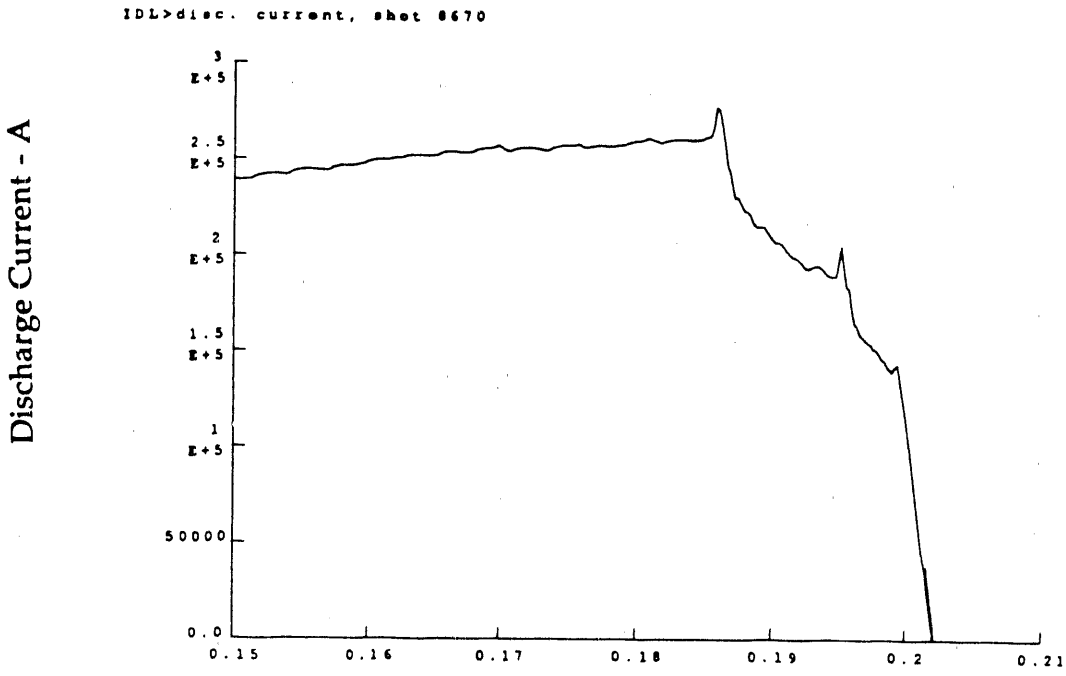

(a) Discharge current with the three disruptions.

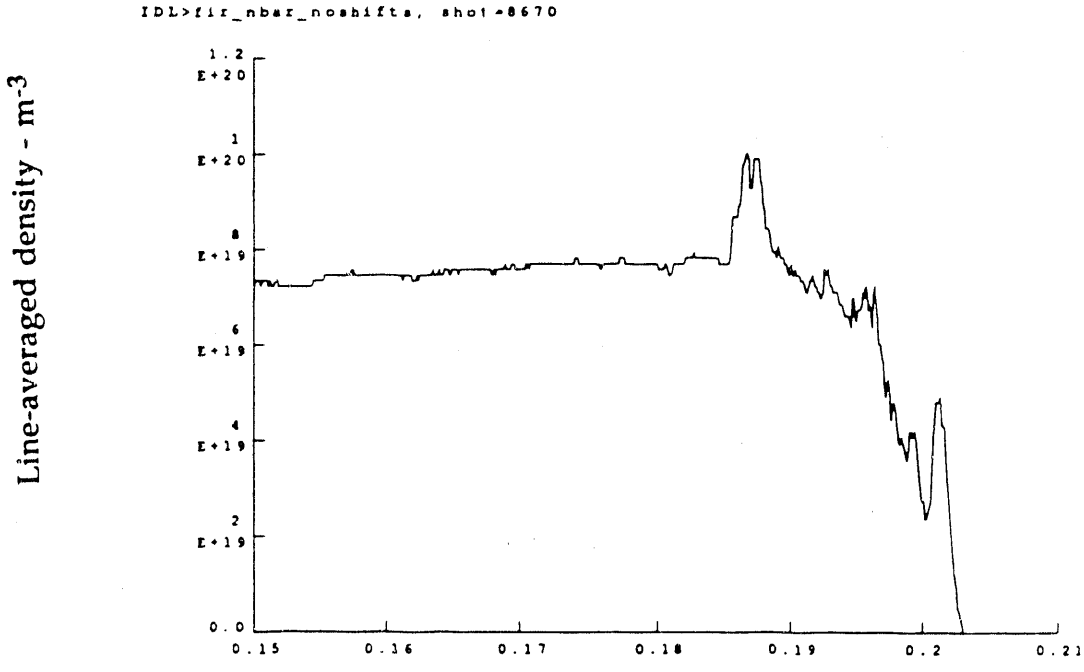

(b) Line-averaged density. Note that poloidal symmetry is broken following the first disruption.

Fig. 7

chord at -11.75 cm deleted

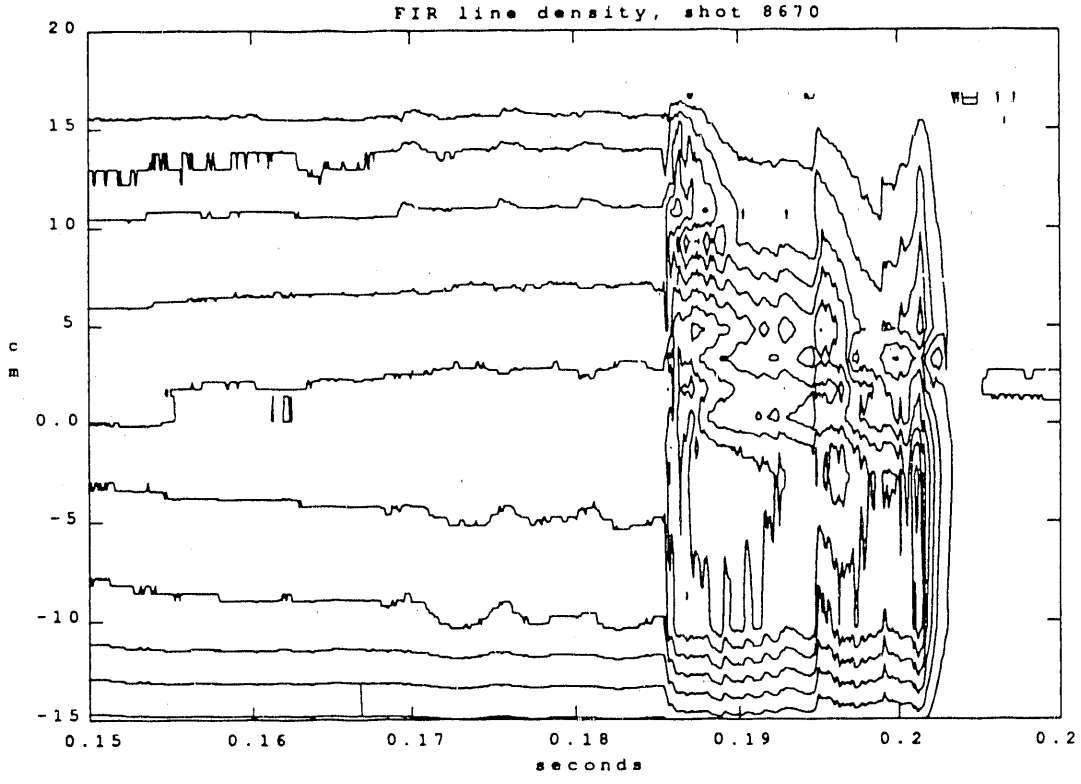

Fig. 8 Chord-averaged density.

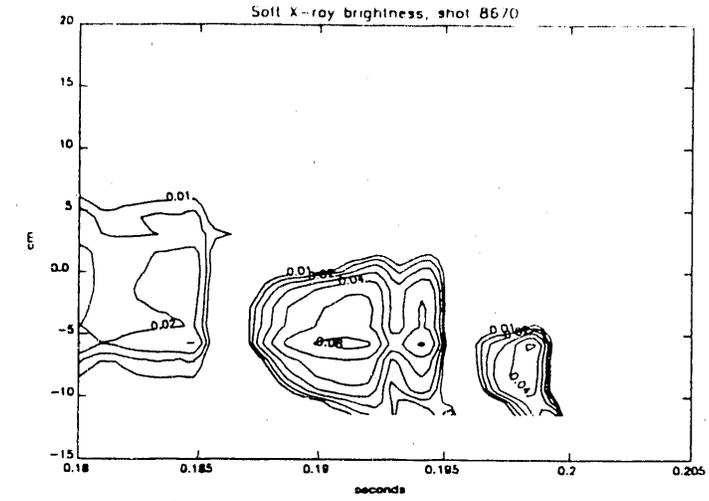

(a) Soft x-rays (chord-averaged)

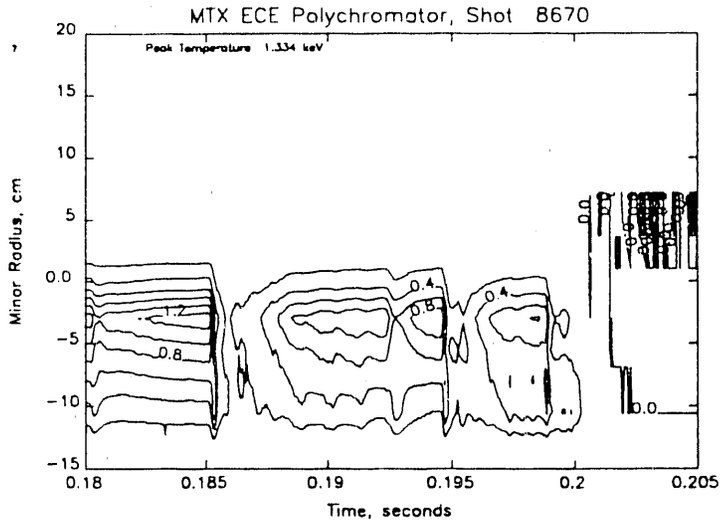

(b) Electron temperature (keV)

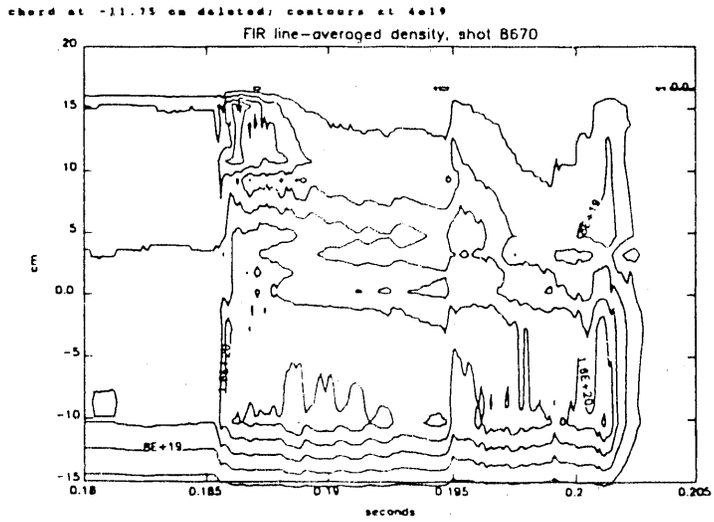

(c) Chord-averaged density

Fig. 9 The disruption

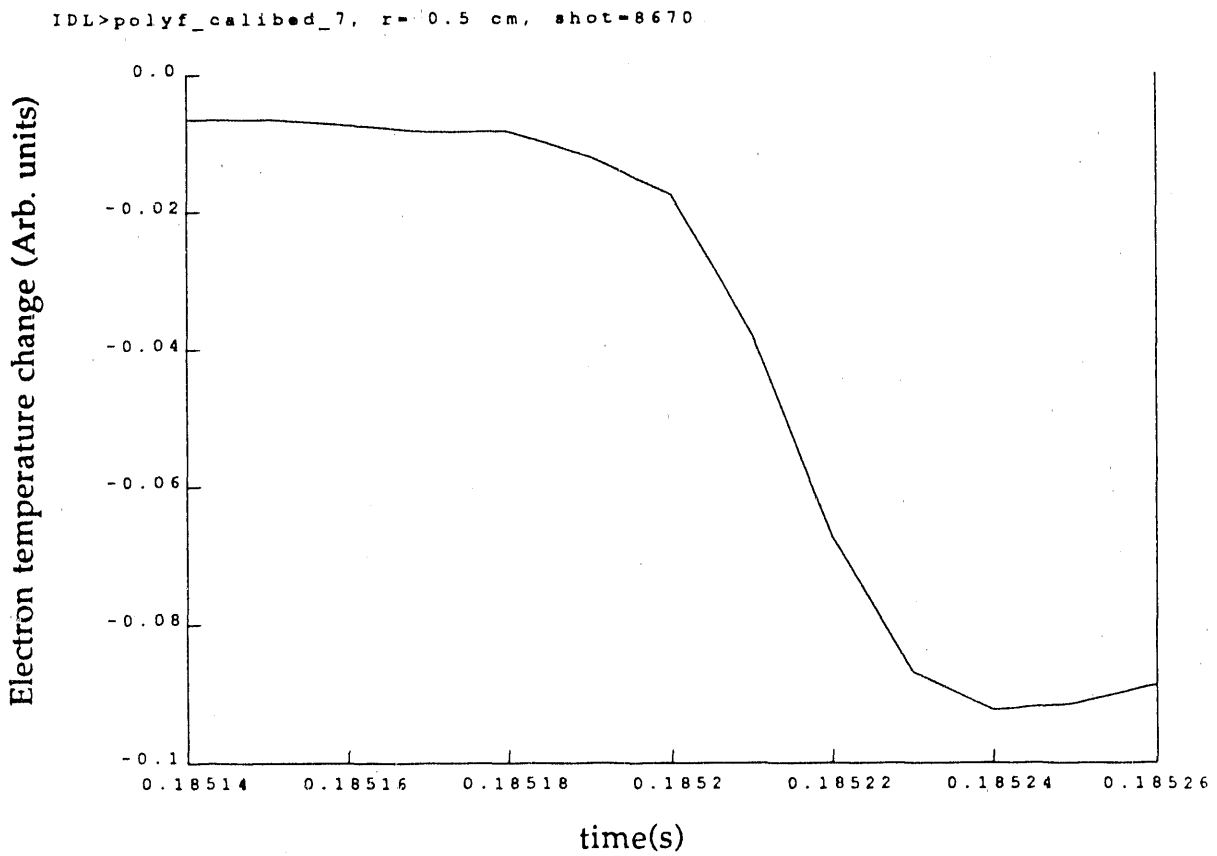

Fig. 10 Electron temperature change at r = -0.5 cm during the first disruption.

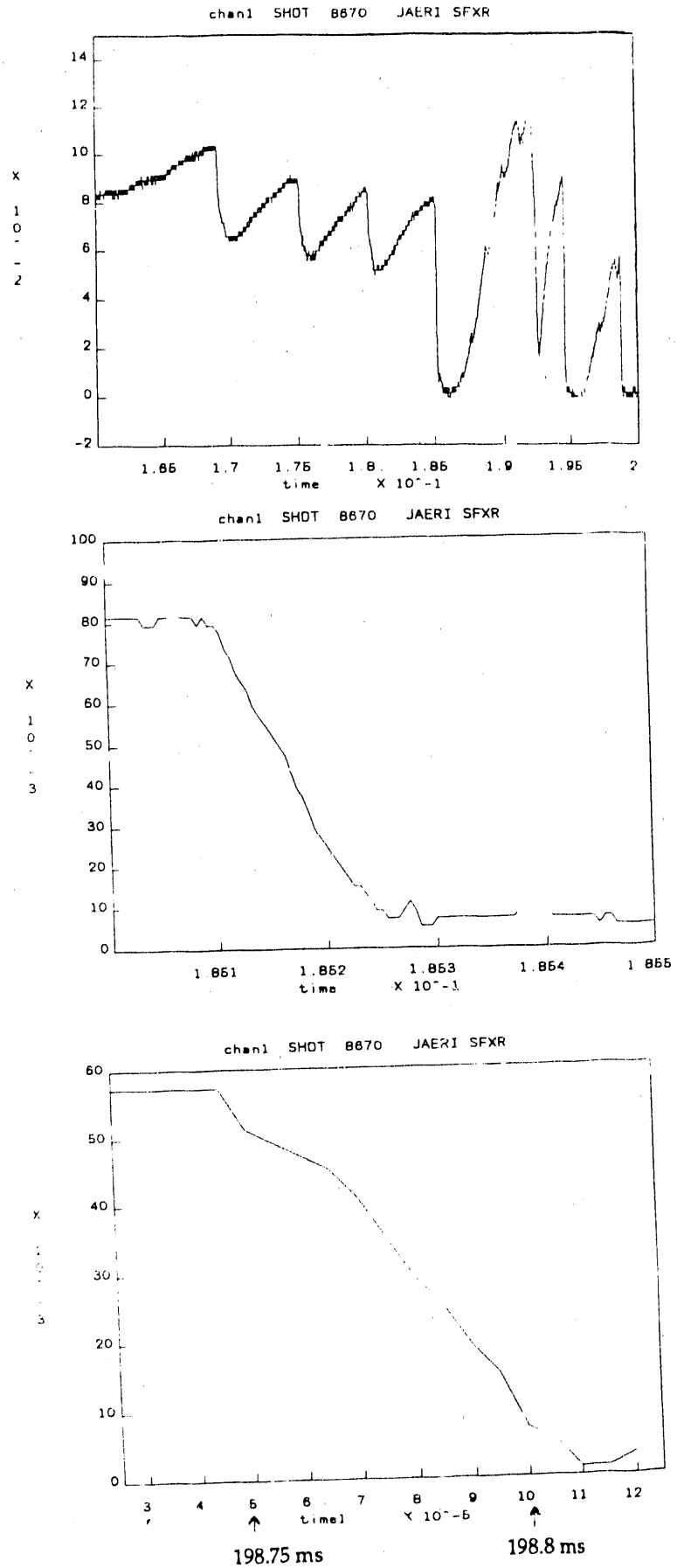

Fig. 11 Fast (JAERI) soft x-rays. (Averaged over plasma.)

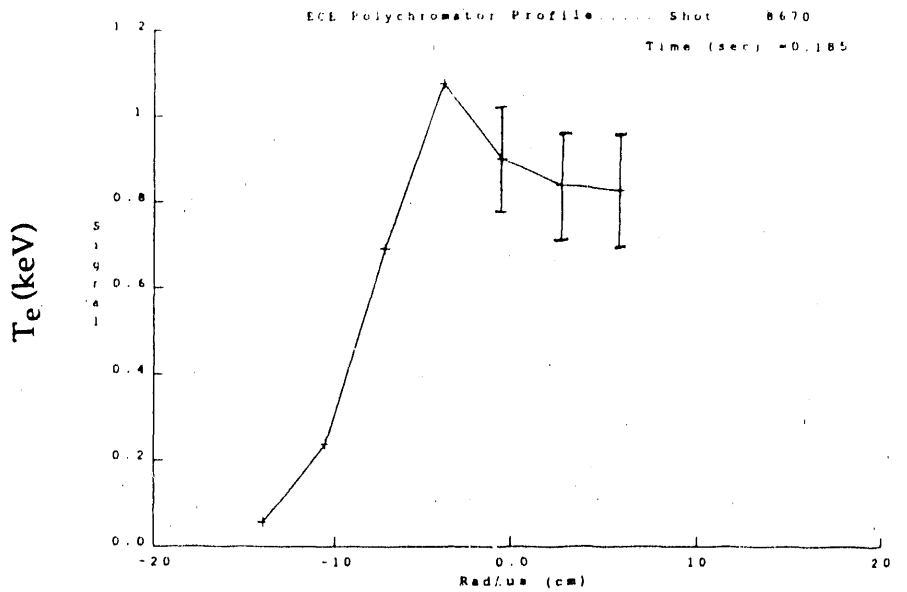

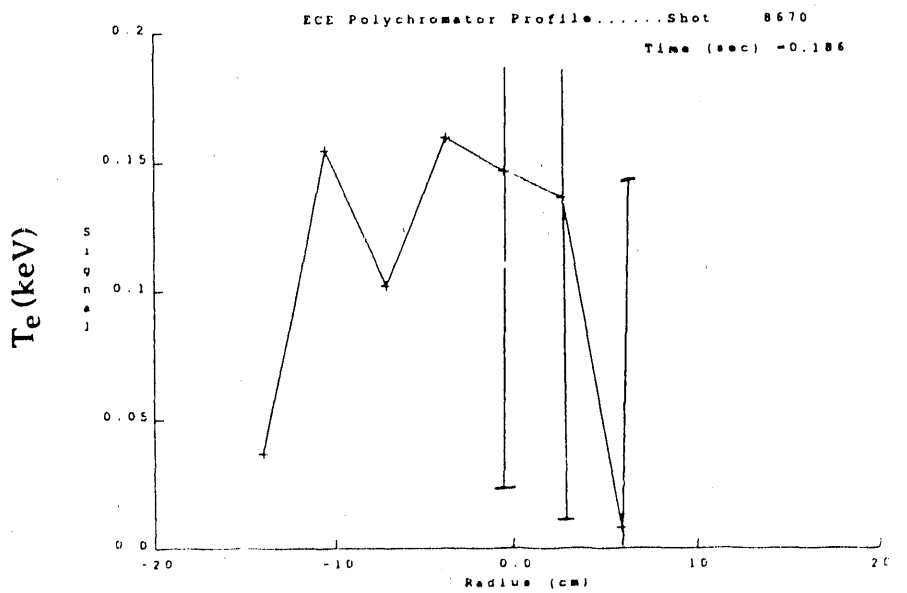

Fig. 12 T_e profiles before and after the disruption. The three channels with error bars had low sensitivity and corresponding large bit size.

END

DATE FILMED

01 / 18 / 91